

Fermi Bubble: Giant Gamma-ray Bubble structure in the Milky Way

Meng Su

Institute for Theory and Computation, Harvard-Smithsonian Center for Astrophysics, 60 Garden Street, Cambridge, MA 02138 USA

Data from the *Fermi*-LAT reveal two large gamma-ray bubbles, extending 50 degrees above and below the Galactic center, with a width of about 40 degrees in longitude. The gamma-ray emission associated with these bubbles has a significantly harder spectrum ($dN/dE \sim E^{-2}$) than the inverse Compton (IC) emission from electrons in the Galactic disk, or the gamma-rays produced by decay of pions from proton-ISM collisions. There is no significant spatial variation in the spectrum or gamma-ray intensity within the bubbles, or between the north and south bubbles. The bubbles are spatially correlated with the hard-spectrum microwave excess known as the *WMAP* haze; the edges of the bubbles also line up with features in the *ROSAT* X-ray maps at 1.5 – 2 keV. We argue that these Galactic gamma-ray bubbles were most likely created by some past large episode of energetic events in the Galactic center.

1. Introduction

Two giant gamma-ray lobes, we referred as the *Fermi* bubble, have been discovered in our Galaxy from the *Fermi*-LAT data [1]. The bubble structure extends ~ 50 degrees above and below the Galactic center (GC), with a width of ~ 40 degrees in longitude. The north and south bubbles are symmetric with respect to the galactic plane and the minor axis of the galactic disk, and both have relatively sharp edges. The gamma-ray signal reveals similar morphology to the previously discovered structures in microwave, named *WMAP* haze [2, 3]. We also found well allocated features in the *ROSAT* X-ray maps at 1.5 keV towards the GC.

As we will discuss, the sharp edges, bilobular shape, and apparent centering on the GC of these structures suggest that they were created by some large episode of energy injection in the GC, such as a past accretion onto the central supermassive black hole, or a nuclear starburst in the last ~ 10 Myr.

2. Fermi Bubbles

The *Fermi* Large Area Telescope (LAT; see [4]; [5]; as well as the *Fermi* homepage¹) is a pair-conversion telescope with a wide field of view, and covers the energy range from about 30 MeV to 300 GeV. For our analysis, the detected events have been binned into a full sky map with different energy range using HEALPix.² We construct maps of front-converting and back-converting events separately, smooth to a common PSF, and then combine them [1]. We use the

Fermi-LAT 1-year Point Source Catalog,³ and subtract each point source from the maps in each energy bin, using estimates of the PSF from the *Fermi* science tools. Each map has been smoothed after point source subtraction by the appropriate kernel to obtain a Gaussian PSF of 2° FWHM (Please see [1, 6] for details of data analysis including map construction, smoothing, masking etc.)

The dominant galactic gamma-rays originate from π^0 gammas produced by CR protons interacting with the ISM. We use the Schlegel, Finkbeiner, & Davis (SFD) map of Galactic dust, based on far IR data [7], as the spatial tracers of the ISM. In Figure 1, we show the full sky *Fermi* maps at 1 – 5 GeV and 5 – 50 GeV after subtracting the SFD dust and a simple disk model to best reveal the *Fermi* bubble features. The purpose of this disk template subtraction is to reveal the structure deeper into the plane, and allow a harder color stretch. The disk model mostly removes the IC gamma-rays produced by cosmic ray electrons interacting with the interstellar radiation field (ISRF) including CMB, infrared, and optical photons, such electrons are thought to be mostly injected in the Galactic disk by supernova shock acceleration before diffusing outward [1].

Although photon Poisson noise is much greater in the 5 – 50 GeV map, we identify the *Fermi* bubble structure with similar morphology to the structure in the 1 – 5 GeV map, both present the north/south symmetry with respect to the Galactic plane. If the *Fermi* bubble constitute the projection of a three dimensional two-bubble structure symmetric to the Galactic plane and the minor axis of the Galactic disk, taking the distance to the GC $R_\odot = 8.5$ kpc, the bubble centers are approximately 10 kpc away from us and ~ 5 kpc above and below the Galactic center, extending up to roughly 10 kpc as the most distant edge from

¹<http://fermi.gsfc.nasa.gov/>

²HEALPix software and documentation can be found at <http://healpix.jpl.nasa.gov>, and the IDL routines used in this analysis are available as part of the IDLUTILS product at <http://sdss3data.lbl.gov/software/idlutils>.

³Available from <http://fermi.gsfc.nasa.gov/ssc/data>

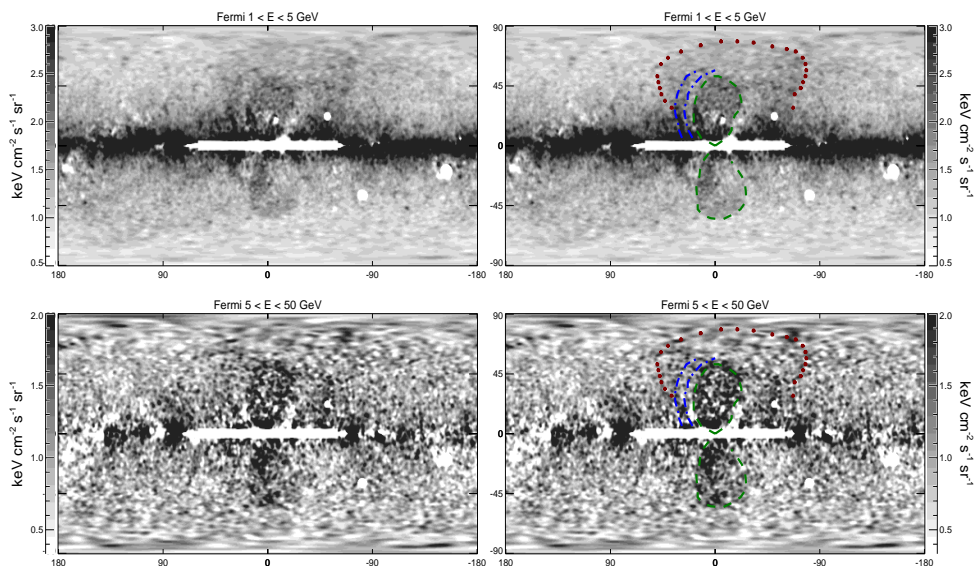


Figure 1: Full sky residual maps after subtracting the SFD dust and disk templates from the *Fermi*-LAT 1.6 year gamma-ray maps in two energy bins. Point sources are subtracted, and large sources, including the inner disk ($-2^\circ < b < 2^\circ$, $-60^\circ < \ell < 60^\circ$), have been masked. Two large bubbles are seen (spanning $-50^\circ < b < 50^\circ$) in both cases. *Right panels*: are the same as the *left panels* but with apparent large scale features marked with color lines overlotted on the maps. Green dashed circles above and below the Galactic plane indicate the approximate edges of the north and south *Fermi* bubble respectively. Two blue dashed arcs mark the inner (dimmer) and outer (brighter) edges of the *northern arc* – a feature in the northern sky outside the north bubble. The red dotted line approximately marks the edge of *Loop I* [1].

GC has $|b| \sim 50^\circ$. No structures like this appear in GALPROP models, and in fact GALPROP is often run with a box-height smaller than this. Because the structures are so well centered on the GC, they are unlikely to be local.

In the *right* panels of Figure 1, we illustrate the edges of the *Fermi* bubble and some other features. We find that the *Fermi* bubble have distinct sharp edges, rather than smoothly falling off as modeled in [6]. Besides the two bubbles symmetric with respect to the Galactic plane, we find one giant *northern arc* that embraces half of the north bubble, that extends from the disk up to $b \sim 50$, with ℓ ranging from roughly -40° to 0° . It has a brighter and sharper outer edge in the 1–5 GeV map. On a even larger scale, we identify a fainter structure extended up to $b \sim 80^\circ$, with ℓ ranging from roughly -80° to 50° which corresponds to the *North Polar Spur* emission associated with *Loop I* [9]. In the 1–5 GeV map, we also identify a “donut-like” structure in the south sky with b ranging from roughly -35° to 0° and ℓ from roughly 0° to 40° .

To study the sharp edges of the bubbles at high latitude more carefully, we examine the (projected) intensity profiles along arcs of great circles passing through the estimated centers of the north and south bubbles (more details see [1]). The results are shown in Figure 2 for the averaged $(1-2) + (2-5)$ GeV maps. In both north and south bubbles, the edges are clearly visible; in the south, this is true even before

any templates are subtracted. For both of the north and south bubbles, no significant edge-brightening or limb-brightening of the bubbles is apparent from the profiles, the flux is fairly uniform inside the bubbles.

In order to reveal the energy spectrum of the *Fermi* bubble, and quantitatively study the intensity flatness of the bubble interiors, we have performed a careful regression template fitting in [1]. We maximize the Poisson likelihood of a simple diffuse emission model involving 5-templates. In this model, we include the SFD dust map as a tracer of π^0 emission which is dominant (or nearly so) at most energies on the disk and significant even at high latitudes, the simple disk model, the bubble template, the *Loop I* template, and a uniform background as templates to weight the *Fermi* data properly. We compute the Poisson log likelihood for different choice of templates in [1]. We refer to Appendix B of [6] for more details of the likelihood analysis. The fitting is done with regions of $|b| > 30^\circ$. In Figure 3, we show spectra for π^0 emission, bremsstrahlung and inverse Compton scattering calculated using a sample GALPROP model (tuned to match locally measured protons and anti-protons as well as locally measured electrons at $\sim 20-30$ GeV), as an indication of the expected spectral shapes. The spectra for the SFD and the simple disk template reasonably match the model expectations. The dust map mostly traces the π^0 emission, and the simple disk model resem-

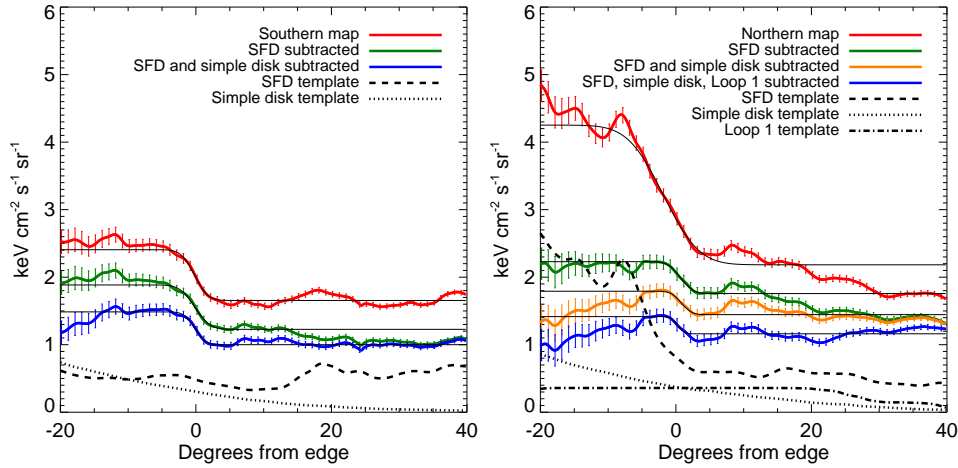


Figure 2: Intensity as a function of radial distance from the bubble edge, averaged over great circle arcs intersecting the bubble center and lying at $|b| > 28^\circ$. Results are shown for (left) the southern bubble, and (right) the northern bubble, for the averaged 1 – 2 and 2 – 5 GeV maps. Different lines show the results at different stages of the template regression procedure and the corresponding errors are plotted (see [1] of the error analysis).

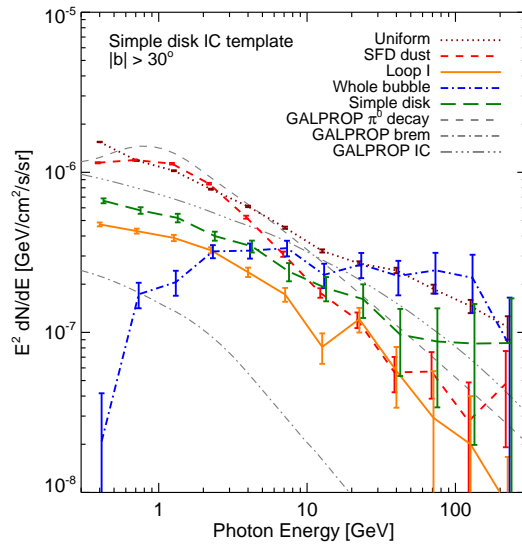


Figure 3: Correlation spectra for the 5-template fit employing a simple disk model for the IC (and to a lesser degree bremsstrahlung) emission from supernova-shock-accelerated electrons. The SFD-correlated spectrum is shown by the red short-dashed line which roughly traces π^0 emission (the gray dashed line indicates a GALPROP prediction for π^0 emission). The disk-correlated emission is shown by the green dashed line, which traces the soft IC (gray triple-dot-dashed line) and bremsstrahlung (gray dot-dashed line) component. The spectrum of the uniform emission, which traces the isotropic background (including possible cosmic-ray contamination), is shown as a dotted brown line. The solid orange line indicates the spectrum of emission correlated with *Loop 1*, which has a similar spectrum to the disk-correlated emission. Finally, the blue dot-dashed line shows the spectrum correlated with the *Fermi* bubble template. The fitting is done over the $|b| > 30^\circ$ region.

bles a combination of IC and bremsstrahlung emission. The spectrum for emission correlated with the *Fermi* bubble is clearly significantly harder than either of these components, consistent with a *flat* spectrum in $E^2 dN/dE$. This fact coupled with the distinct spatial

morphology of the *Fermi* bubble indicates that the IC bubbles are generated by a *separate* electron component. We also note that the spectrum of the bubble template falls off significantly at energy less than 1 GeV. This feature is robust with respect to the choice

of templates.

3. Comparison with *ROSAT* X-ray Features

The *ROSAT* all-sky survey provides full-sky images with FWHM 12' at energies from 0.5 – 2 keV.⁴ We compare the morphology of the X-ray features in *ROSAT* 1.5 keV map with the edges of the *Fermi* bubble in detail in [1]. The limb brightened X-ray features align with the edges of both the north and south *Fermi* bubble. Hints of the whole north bubble are also visible in *ROSAT*, as well as two sharp edges in the south that trace the south *Fermi* bubble close to the disk. We subtract the *ROSAT* 1.0 keV soft X-ray map from the 1.5 keV map to clean up the foreground emission. We find that the more extended *Loop I* feature has a softer spectrum than the X-ray features associated with the bubble edges, and is largely removed after subtraction. The dominant edges features strikingly overlap with the edges of the *Fermi* bubble at lower latitude. No other noticeable large scale features appear in the residual X-ray map which do not appear in the gamma-rays. The appearance of the X-ray edges in the *ROSAT* 1.5 keV map, coincident with the *Fermi* bubble edges, strongly supports the physical reality of these sharp edges.

4. Comparison with WMAP Microwave Haze

The *WMAP* haze is the residual remaining in *WMAP* microwave data after regressing out contributions from thermal dust, free-free, and “soft synchrotron” traced by the Haslam 408 MHz radio survey [9]. Therefore, it is by construction harder than the Haslam-correlated emission. In [1] we performed a detailed morphological comparison of the south *Fermi* bubble at 1 – 5 GeV with the southern part of the *WMAP* microwave haze at 23 GHz (K-band). The edge of the *Fermi* bubble, marked in green dashed line in the *top right* and *lower right* panels, closely traces the edge of the *WMAP* haze. The smaller latitudinal extension of the *WMAP* haze may be due to the decay of the magnetic field strength with latitude. These striking morphological similarities between the *WMAP* microwave haze and *Fermi* gamma-ray bubble can be readily explained if the *same* electron CR population is responsible for both excesses, with the electron CRs interacting with the galactic magnetic

field to produce synchrotron, and interacting with the ISRF to produce IC emission.

5. Summary and Discussions

We have identified two large gamma-ray bubbles in *Fermi* maps containing 1.6 years of data. They have approximately uniform surface brightness with sharp edges, neither limb brightened nor centrally brightened, and are nearly symmetric about the Galactic plane. The bubbles extend to 50° above and below the Galactic center, with a maximum width of about 40° in longitude. These “*Fermi* bubble” have a spatial morphology similar to the *WMAP* microwave haze [2, 3]. The *ROSAT* soft X-ray 1.5 keV map also reveals hard-spectrum features that align well with the edges of the *Fermi* bubble. The similarities of the morphology and hard spectrum strongly suggest that the *WMAP* haze and the *Fermi* bubble share a common origin.

To better reveal the bubble structures, we use spatial templates to regress out known emission mechanisms. We found that the *Fermi* bubble have an energy spectrum of $dN/dE \sim E^{-2}$, significantly harder than other gamma-ray components. Both the morphology and spectrum are consistent with the two bubbles having the same origin and being the IC counterpart to the electrons which generate the microwave haze seen in *WMAP*. Even setting aside the *WMAP* haze, the *Fermi* bubble are unlikely to originate from excess π^0 emission, and the *ROSAT* data suggest that the bubbles are hot and underdense rather than overdense. The morphology of the *Fermi* bubble strongly *disfavor* the hypothesis that a significant fraction of the high energy gamma rays observed by *Fermi* in the bubble region are photons directly produced by dark matter annihilation.

The *Fermi* bubble structures were likely created by some large episode of energy injection in the GC, such as a past accretion event onto the central supermassive black hole, or a nuclear starburst in the last ~10 Myr. Jets originating from AGN activity can potentially accelerate CR electrons to high energies, and transport them rapidly away from the GC. An alternate source for the large required energy injection is a nuclear starburst (see [1] for more discussion on the origin of *Fermi* bubbles).

The *eROSITA*⁵ and *Planck*⁶ experiments will provide improved measurements of the X-rays and microwaves, respectively, associated with the *Fermi* bubble, and so may help discriminate between these scenarios.

⁴<http://hea-www.harvard.edu/rosat/rsdc.html>

⁵<http://www.mpe.mpg.de/heg/www/Projects/EROSITA/main.html>

⁶<http://www.rssd.esa.int/index.php?project=Planck>

References

- [1] M. Su, T. R. Slatyer, D. P. Finkbeiner, *ApJ* **724**, 1044 (2010).
- [2] Finkbeiner, D. P. 2004, *Astrophys. J.*, 614, 186
- [3] Dobler, G., & Finkbeiner, D. P. 2008, *Astrophys. J.*, 680, 1222
- [4] Gehrels, N., & Michelson, P. 1999, *Astropart. Phys.*, 11, 277
- [5] Atwood, W. B., et al. 2009, *Astrophys. J.*, 697, 1071
- [6] Dobler, G., Finkbeiner, D. P., Cholis, I., Slatyer, T., & Weiner, N. 2010, *Astrophys. J.*, 717, 825
- [7] Schlegel, D. J., Finkbeiner, D. P., & Davis, M. 1998, *Astrophys. J.*, 500, 525
- [8] Grenier, I. A., Casandjian, J., & Terrier, R. 2005, *Science*, 307, 1292
- [9] Haslam, C. G. T., Salter, C. J., Stoffel, H., & Wilson, W. E. 1982, *Astron. Astrophys. Supp.*, 47, 1
- [10] Abdo, A. A., et al. 2010, *Phys. Rev. Lett.*, 104, 101101